GW with linearized augmented plane waves extended by high-energy local orbitals

Hong Jiang[1,*] and Peter Blaha[2]

[1]*Beijing National Laboratory for Molecular Sciences, College of Chemistry and Molecular Engineering, Peking University, 100871 Beijing, China*

[2]*Institute of Materials Chemistry, Vienna University of Technology, Getreidemarkt 9/165-TC, A-1060 Vienna, Austria*

(Received 1 September 2015; revised manuscript received 19 February 2016; published 14 March 2016)

Many-body perturbation theory in the *GW* approximation is currently the most accurate and robust first-principles approach to determine the electronic band structure of weakly correlated insulating materials without any empirical input. Recent *GW* results for ZnO with more careful investigation of the convergence with respect to the number of unoccupied states have led to heated debates regarding the numerical accuracy of previously reported *GW* results using either pseudopotential plane waves or all-electron linearized augmented plane waves (LAPWs). The latter has been arguably regarded as the most accurate scheme for electronic-structure theory for solids. This work aims to solve the ZnO puzzle via a systematic investigation of the effects of including high-energy local orbitals (HLOs) in the LAPW-based *GW* calculations of semiconductors. Using ZnO as the prototypical example, it is shown that the inclusion of HLOs has two main effects: it improves the description of high-lying unoccupied states by reducing the linearization errors of the standard LAPW basis, and in addition it provides an efficient way to achieve the completeness in the summation of states in *GW* calculations. By investigating the convergence of *GW* band gaps with respect to the number of HLOs for several other typical examples, it was found that the effects of HLOs are highly system-dependent, and in most cases the inclusion of HLOs changes the band gap by less than 0.2 eV. Compared to its effects on the band gap, the consideration of HLOs has even stronger effects on the *GW* correction to the valence-band maximum, which is of great significance for the *GW* prediction of the ionization potentials of semiconductors. By considering an extended set of semiconductors with relatively well-established experimental band gaps, it was found that in general using a HLO-enhanced LAPW basis significantly improves the agreement with experiment for both the band gap and the ionization potential, and overall the partially self-consistent GW_0 approach based on the generalized gradient approximation gives an optimal performance.

DOI: 10.1103/PhysRevB.93.115203

I. INTRODUCTION

Since the seminal work by Hybertsen and Louie [1] and Godby, Schlüter, and Sham [2] in the 1980s, many-body perturbation theory in the *GW* approximation, often implemented as a correction to Kohn-Sham density-functional theory in the local-density approximation (LDA) or the generalized-gradient approximation (GGA), has established itself as the most accurate and robust first-principles approach to calculate the electronic band structure of weakly correlated insulating materials without any empirical input [3–5]. Most of the early implementations of *GW* for solids are based on pseudopotentials (PP) and a plane-wave basis [1,2,6,7]. Recently, there have been several implementations of *GW* based on the projector augmented wave method (PAW) [8,9], which is an all-electron approach but with the frozen-core approximation (FCA), the linearized augmented plane waves (LAPW), or the muffin-tin orbital (LMTO) methods [10–18]. The effects of using the PP approximation in *GW* calculations have been carefully analyzed in a series of studies [11,16,19–21], and now it seems to be well accepted that only when semicore states that belong to the same shell as valence electrons are treated as "valence" can the PP approximation provide comparable accuracy to all-electron approaches for *GW* calculations.

Another issue that has caused heated debates in the *GW* community recently is the convergence of the *GW* band gap of ZnO with respect to the number of unoccupied bands [22–25]. ZnO, an apparently simple semiconductor, has been one of the well-known "difficult" systems for which one-shot or partially self-consistent *GW* treatments based on LDA/GGA, denoted as G_0W_0 and GW_0 [26], respectively, still give a significantly underestimated band gap [27–29]. The latter was often attributed to significantly overestimated interaction between Zn 3*d* and O 2*p* states by LDA/GGA. Indeed, by using a single-particle Hamiltonian with an improved description of semicore *d*-states [i.e., that from hybrid functionals [28,30,31] or the exact-exchange optimized effective potential (OEP) approach [32]] as the input for G_0W_0, or using approximate self-consistent *GW* [33,34], much improved agreement with experiment can be obtained for the band gap of ZnO. It was therefore a big surprise for the community when Shih *et al.* [22] reported the remarkable findings that the widely observed underestimation of the G_0W_0 band gap for ZnO was caused by the ill-convergence of G_0W_0 calculations with respect to the number of unoccupied bands (N_b), and by considering as many as $N_b \sim 3000$ unoccupied bands, the LDA-based G_0W_0 gives a gap of about 3.4 eV, which is almost 1 eV larger than previous published G_0W_0 gaps [27–29]. Shih *et al.*'s findings, however, have a loophole: the frequency dependency of the dielectric function was treated by the Hybertsen-Louie (HL) generalized plasmon-pole (GPP) model [1], which depends on the *f*-sum rule. A later study by Stankovski *et al.* [23] shows that the slow convergence of the G_0W_0 band gap with respect to N_b is indeed related to the use of the HL-GPP mode; when using the contour deformation (CD) approach [2], which is arguably a more accurate treatment of the frequency

*Author to whom all correspondence should be addressed: jianghchem@pku.edu.cn

dependence than the GPP model, the convergence with respect to N_b can be readily achieved, and the converged G_0W_0 band gap is only slightly larger than previously reported values. To solve the ZnO puzzle, Friedrich *et al.* [24] performed a detailed investigation of ZnO using GW implemented in the LAPW basis. They found that when using the "standard" LAPW basis, the G_0W_0 band gap of ZnO converges rather quickly as a function of N_b. The convergence, however, becomes much slower when hundreds of additional high-energy local orbitals (HLOs), i.e., basis functions that contribute only within the muffin-tin spheres [35], are included to improve the quality of the LAPW basis to represent high-lying unoccupied states, and the final N_b-converged G_0W_0 band gap of ZnO obtained from an extrapolation to an infinite number of unoccupied bands is about 3.0 eV, which is about 0.4–0.9 eV larger than previously reported values, but still about 0.4 eV smaller than the value reported by Shih *et al.* [22].

The LAPW basis is often regarded as the most accurate one to describe the electronic structure of solids [36], and the results based on LAPW, either at the DFT level or at the GW level, are often taken as benchmark to validate other more approximate treatments [21]. Considering the far-reaching implications of Friedrich *et al.*'s findings [24], it is important to investigate the issue in more detail. In particular, we address several open questions that are not answered in the previous publications: (i) What is the real origin of the slow N_b convergence of the G_0W_0 band gap in ZnO? (ii) Is such slow convergence a general feature of GW calculations or is it system-dependent? (iii) What are the effects of HLOs on the GW correction to the valence-band maximum, which is crucial to obtain accurate ionization potentials of semiconductors [37–42]? We address these issues based on the latest version of the GAP (GW with augmented plane waves) code [18], which has been extended to support the use of a LAPW basis with an arbitrary number of LOs per angular momentum channel (l). The latter has been recently implemented in the WIEN2K code [43] as required for the accurate evaluation of NMR chemical shifts in the LAPW framework [44,45]. It should be noted that the importance of local orbitals for an accurate description of high-lying unoccupied states has been addressed by several authors in other contexts [46–49], and that the effects of including HLOs in the GW calculations for Si were already investigated by Blügel and co-workers in 2006 [14].

This paper is organized as follows. The next section presents a short overview on the implementation of the GW approach in the LAPW basis (see Ref. [18] for more details). In Sec. III we first present a systematic investigation of ZnO, which confirms the previously reported results and further clarifies the origin of the ZnO puzzle. We then consider several representative semiconductors and insulators to show that the effects of HLOs are highly system-dependent. Finally, we present numerically well-converged G_0W_0 and GW_0 results for a set of prototypical systems, including both band gaps and ionization potentials, which can be used as benchmark data for further theoretical development. Section IV summarizes the main findings of this work and closes the paper with some general remarks.

II. THEORY AND METHOD

A. The G_0W_0 approach

Quasiparticle energies ($\varepsilon_{n\mathbf{k}}^{(\mathrm{QP})}$) in the G_0W_0 approach are calculated by first-order perturbation correction to KS-DFT single-particle energies $\varepsilon_{n\mathbf{k}}$,

$$\varepsilon_{n\mathbf{k}}^{(\mathrm{QP})} = \varepsilon_{n\mathbf{k}} + Z_{n\mathbf{k}}\langle\psi_{n\mathbf{k}}|\Sigma_{\mathrm{xc}}(\varepsilon_{n\mathbf{k}}) - V_{\mathrm{xc}}|\psi_{n\mathbf{k}}\rangle, \tag{1}$$

where V_{xc} is the approximate exchange-correlation potential in KS-DFT, $\psi_{n\mathbf{k}}(\mathbf{r})$ are KS orbital wave functions, and $Z_{n\mathbf{k}}$ is the QP renormalization factor given by

$$Z_{n\mathbf{k}} = \left[1 - \left(\frac{\partial}{\partial\epsilon}\langle\psi_{n\mathbf{k}}|\Sigma_{\mathrm{xc}}(\epsilon)|\psi_{n\mathbf{k}}\rangle\right)_{\epsilon=\varepsilon_{n\mathbf{k}}}\right]^{-1}. \tag{2}$$

By introducing an auxiliary basis $\chi_i^{\mathbf{q}}(\mathbf{r})$ that can accurately represent products of two Kohn-Sham orbitals, often termed the product basis,

$$\psi_{n\mathbf{k}}(\mathbf{r})\,\psi^*_{m\mathbf{k}-\mathbf{q}}(\mathbf{r}) = \sum_i M^i_{nm}(\mathbf{k},\mathbf{q})\,\chi_i^{\mathbf{q}}(\mathbf{r}), \tag{3}$$

with the expansion coefficients $M^i_{nm}(\mathbf{k},\mathbf{q})$ given by

$$M^i_{nm}(\mathbf{k},\mathbf{q}) \equiv \int_\Omega \left[\chi_i^{\mathbf{q}}(\mathbf{r})\,\psi_{m\mathbf{k}-\mathbf{q}}(\mathbf{r})\right]^*\psi_{n\mathbf{k}}(\mathbf{r})d\mathbf{r}, \tag{4}$$

where Ω indicates the volume of the unit cell, the diagonal elements of the GW self-energy in terms of KS orbitals read

$$\langle\psi_{n\mathbf{k}}|\Sigma_{\mathrm{xc}}(\omega)|\psi_{n\mathbf{k}}\rangle = N_c^{-1}\sum_{\mathbf{q}}\sum_m\sum_{i,j}\frac{i}{2\pi}\int_{-\infty}^{\infty}d\omega' e^{i\omega'\eta} \times\frac{\left[M^i_{nm}(\mathbf{k},\mathbf{q})\right]^* W_{ij}(\mathbf{q},\omega')M^j_{nm}(\mathbf{k},\mathbf{q})}{\omega+\omega'-\varepsilon_{m\mathbf{k}-\mathbf{q}}}, \tag{5}$$

where N_c is the number of $\mathbf{q}$-mesh points equally spaced in the Brillouin zone, and η is a positive infinitesimal. $W_{ij}(\mathbf{q},\omega)$ are the matrix elements in the product basis representation of the dynamically screened Coulomb interaction, defined as

$$W(\mathbf{r},\mathbf{r}';\omega) = \int\varepsilon^{-1}(\mathbf{r},\mathbf{r}'';\omega)v(\mathbf{r}''-\mathbf{r}')d\mathbf{r}'', \tag{6}$$

where $\varepsilon^{-1}(\mathbf{r},\mathbf{r}';\omega)$ is the inverse dielectric function and v is the bare Coulomb interaction.

B. GW in the LAPW basis

The LAPW basis is characterized by its mixed feature: it behaves atomiclike in the region around each nucleus that is defined by the so-called muffin-tin (MT) radius R_{MT}, and plane-wave-like in the interstitial region (I) between nuclei,

$$\phi^{\mathbf{k}}_{\mathbf{G}}(\mathbf{r}) = \begin{cases}\sum_{lm}[A_{\alpha lm}(\mathbf{k}+\mathbf{G})u_{\alpha l}(r^\alpha;E_{\alpha l}) + B_{\alpha lm}(\mathbf{k}+\mathbf{G})\dot{u}_{\alpha l}(r^\alpha;E_{\alpha l})]\,Y_{lm}(\hat{\mathbf{r}}^\alpha), & r^\alpha < R^\alpha_{\mathrm{MT}},\\ \frac{1}{\sqrt{\Omega}}e^{i(\mathbf{k}+\mathbf{G})\cdot\mathbf{r}}, & \mathbf{r}\in I,\end{cases} \tag{7}$$

with $\mathbf{r}^\alpha \equiv \mathbf{r} - \mathbf{r}_\alpha$, and $R^\alpha_{\rm MT}$ is the MT radius of the αth atom. $u_{\alpha l}(r^\alpha; E_{\alpha l})$ are the solutions of the radial Schrödinger equation at a fixed reference energy $E_{\alpha l}$ in the spherical potential of the respective MT sphere, and $\dot{u}_{\alpha l}(r^\alpha; E_{\alpha l})$ is its energy derivative. The expansion coefficients $A_{\alpha lm}(\mathbf{k}+\mathbf{G})$ and $B_{\alpha lm}(\mathbf{k}+\mathbf{G})$ are determined from the continuity of the basis functions and their first derivatives at the boundary of the MT spheres. To improve the description of semicore states (e.g., $3s$ and $3p$ states in $3d$-transition-metal atoms), the LAPW basis can be supplemented by the so-called local orbitals (LOs) that contribute only within the MT spheres [35],

$$\phi^{\rm LO}_{lm}(\mathbf{r}) = \begin{cases} \left[A^{\rm LO}_{\alpha lm} u_{\alpha l}(r^\alpha; E_{\alpha l}) + B^{\rm LO}_{\alpha lm} \dot{u}_{\alpha l}(r^\alpha; E_{\alpha l}) + C^{\rm LO}_{\alpha lm} u_{\alpha l}\left(r^\alpha; E^{(2)}_{\alpha l}\right)\right] Y_{lm}(\hat{\mathbf{r}}^\alpha), & r^\alpha < R^\alpha_{\rm MT}. \\ 0, & \mathbf{r} \in I. \end{cases} \tag{8}$$

Here $u_{\alpha l}(r; E^{(2)}_{\alpha l})$ is a radial wave function evaluated at the reference energy $E^{(2)}_{\alpha l}$ that is close to the energy of semicore states. The coefficients $A^{\rm LO}_{\alpha lm}$, $B^{\rm LO}_{\alpha lm}$, and $C^{\rm LO}_{\alpha lm}$ are uniquely determined by imposing the condition that $\phi^{\rm LO}_{lm}(\mathbf{r})$ is zero in value and slope at the MT sphere boundary and normalized. LOs can be used not only to improve the description of semicore states, but also to greatly improve the accuracy of the treatment of high-lying unoccupied states as needed for accurate calculations of response properties such as NMR chemical shifts in the LAPW framework [44,45]. To systematically improve the completeness of LOs without suffering from the linear dependence problem, Laskowski *et al.* proposed setting the linearization energies of LOs in such a way that the number of nodes in the radial wave functions of LOs is different and increases one by one (see Ref. [44] for a more detailed description). In this work, we denote the additional number of nodes of the highest LOs with respect to the corresponding valence orbital as $n_{\rm LO}$, which is used as a new parameter that characterizes the accuracy of the LO-enhanced LAPW basis. It is interesting to note that the energies of LOs introduced in this way can be quite large [44,45].

The most important ingredient for the implementation of GW in the LAPW-type basis is the product basis $\chi^{\mathbf{q}}_i(\mathbf{r})$. As detailed in Ref. [18], an optimal product basis in the LAPW framework is the so-called mixed basis, which, in analogy to the mixed feature of the LAPW basis, consists of orthonormalized interstitial plane waves in the interstitial region and atomiclike functions in the MT region. Radial functions for the mixed basis in the MT region are obtained by considering the products of radial functions used in the LAPW basis, i.e., $u_{\alpha l}(r)$ in Eqs. (7) and (8), which are further orthonormalized and screened to eliminate linear dependence. When using a HLO-enhanced LAPW basis, the number of radial functions increases quite substantially, which could also increase the size of the mixed basis dramatically. Fortunately, numerical tests indicate that considering radial functions of LOs with very high energy ($>\sim$20 Ry) has negligible effects on the GW results, and therefore only one or two additional radial functions per l-channel need to be considered for the construction of the mixed basis, which may also significantly increase the total number of MT basis functions per atom, but in a feasible way.

C. Computational details

In this work, two types of numerical results are going to be presented. In the first case, we select a few typical systems, and we perform a systematic investigation on how the G_0W_0 band gap is affected by adding increasingly more HLOs (as characterized by $n_{\rm LO}$), with a small number of $\mathbf{k}$-points ($2\times2\times2$ for ZnO, ZnS, Si, GaN, GaAs, MgO, and NiO, and $2\times2\times3$ for TiO_2). In the second type of calculations, in which the goal is to provide benchmark results, we consider a selected set of prototypical semiconductors and insulators, for which experimental band gaps are relatively well established, and we set all relevant computational parameters to well-converged values. In particular, we use the $6\times6\times6$ $\mathbf{k}$-mesh for systems with a cubic unit cell, and the $6\times6\times4$ $\mathbf{k}$-mesh for systems with the wurtzite (wz) structure. Experimental crystal structures are used in all calculations to facilitate the comparison between theory and experiment. Experimental lattice constants obtained from Ref. [50] and other computational details are collected in Table S1 in the supplemental material [51]. The details on the implementation our GW approach are given in Ref. [18].

We use $n_{\rm LO}=0$ to denote the LAPW basis default in the recent version of WIEN2K [43], which is actually a mixture of the APW+lo basis [52] for the valence states, the ordinary LAPW basis for higher l channels up to $l_{\rm max}=10$, and additional LOs for semicore states if present. By default, we add high-energy local orbitals to the LAPW basis with the angular momentum l up to $l^{\rm LO}_{\rm max} \equiv l^{\rm v}_{\rm max}+1$, with $l^{\rm v}_{\rm max}$ being the largest l of valence orbitals for each element, e.g., $l^{\rm v}_{\rm max}=1$ for O and $l^{\rm v}_{\rm max}=2$ for Zn [44,45]. The energy parameters for the HLOs are set such that higher HLOs have one additional radial node within the atomic sphere [44], and they are listed in Table S1. We have also checked the effects of adding HLOs to the LAPW basis with larger l, and we found that for some systems such as ZnO, $l^{\rm LO}_{\rm max} \equiv l^{\rm v}_{\rm max}+4$ is necessary to obtain numerically well-converged results. For the benchmark results presented below, a correction obtained using $l^{\rm LO}_{\rm max} \equiv l^{\rm v}_{\rm max}+4$ but with a smaller number of $\mathbf{k}$-points, typically $2\times2\times2$ for cubic systems and $2\times2\times1$ for the wurtzite systems (see Table S2 in the supplemental material [51]), is included such that the numerical errors in these results are expected to be smaller than 0.05 eV or better.

We will present GW results in the G_0W_0 and GW_0 schemes, in which Kohn-Sham orbital energies and wave functions obtained using the effective potential in the Perdew-Burke-Ernzerhof (PBE) [53] approximation are used as the input to calculate the one-body Green's function G and the screened Coulomb interaction W. We use the default LAPW basis ($n_{\rm LO}=0$) in the PBE self-consistent-field (SCF) calculations. To check the effects of HLOs on the converged PBE effective potential, we did a PBE SCF calculation for wz-ZnO with one

HLO for l up to $l^{\mathrm{v}}_{\mathrm{max}}+1$, and we found that the PBE band gap changes only slightly from 0.83 to 0.82 eV, which justifies our treatment [54].

In addition to the fundamental band gap, we also investigate the effects of HLOs on the ionization potential [40]. The GW corrected ionization potential for a semiconductor is calculated in terms of

$$I^{(GW)} = I^{(\mathrm{PBE})} - \Delta\mathcal{E}_{\mathrm{VBM}}, \tag{9}$$

where $I^{(\mathrm{PBE})}$ is the ionization potential obtained from the PBE slab model calculation, and $\Delta\mathcal{E}_{\mathrm{VBM}}$ is the GW quasiparticle correction to the valence-band maximum obtained from the GW calculation of the bulk system. The PBE results for IPs are taken directly from Ref. [40]. More details on the GW approach to the ionization potentials of semiconductors have been presented in Ref. [40].

III. RESULTS AND DISCUSSIONS

A. Systematic investigation of ZnO

We first perform a systematic investigation of ZnO, and to simplify the calculations, we consider ZnO in the zinc-blende structure instead of the more stable wurtzite polytype. We note that all GW results presented in this section are obtained with a small $2\times2\times2$ **k**-mesh, which are not converged with respect to the number of **k**-points. The G_0W_0 results for ZnO with the default LAPW basis, as implemented in WIEN2K [43], depend noticeably on the choice of R_{MT} for Zn and O and the value of $RK_{\mathrm{max}} \equiv \mathrm{min}R_{\mathrm{MT}} \times K_{\mathrm{max}}$, which determines the energy cutoff for the interstitial plane waves K_{max}. As shown in Table I, when using different R_{MT} and/or RK_{max}, the number of available bands (n_{max}), including both occupied and unoccupied, that can be used in GW calculations differs quite significantly. For example, n_{max} for the ZnO-3 case [R_{MT}(Zn,O) = (1.7,1.2) Bohr and $RK_{\mathrm{max}} = 9.0$] is four times larger than that of the ZnO-2 case ($R_{\mathrm{MT}} = 2.1$ and 1.5 Bohr for Zn and O, respectively, and $RK_{\mathrm{max}} = 7.0$). Figure 1 shows the convergence of the G_0W_0 band gap of ZnO as a function of the number of additional high-energy local orbitals (n_{LO}) with different LAPW basis parameters. The most remarkable feature is that the G_0W_0 band gap increases significantly as n_{LO} increases and tends to converge for $n_{\mathrm{LO}} \geqslant 5$. When using the default LAPW basis ($n_{\mathrm{LO}} = 0$), different choices of the parameters lead to a noticeably different G_0W_0 band gap (by as much as 0.16 eV). The latter, however, is no longer the case when a large number of high-energy LOs ($n_{\mathrm{LO}} \geqslant 5$) are used, indicating that the former is an artifact caused by the inaccuracy of the default LAPW basis. We also note that treating Zn $3p$ as semicore states by setting a LO basis at the corresponding energy has negligible effects (comparing ZnO-2 and ZnO-4) on the final G_0W_0 results. Overall, by including a large enough number of HLOs, the G_0W_0 band gap for ZnO increases by about 0.5–0.6 eV, which is similar to that reported in Ref. [24].

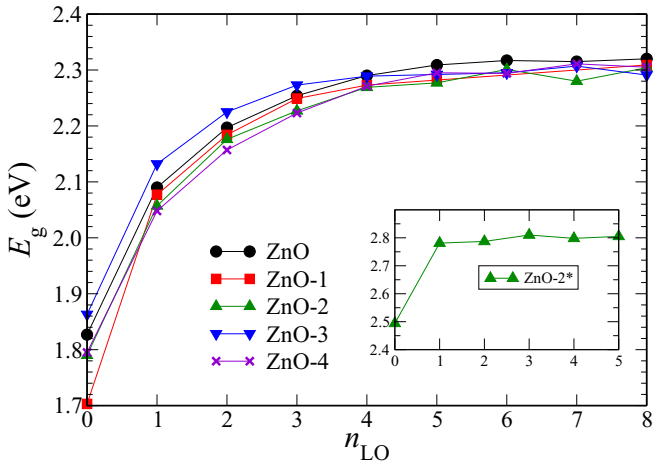

FIG. 1. Convergence of the G_0W_0 band gap of ZnO (using $N_k = 2\times2\times2$) as a function of the number of additional high-energy local orbitals (n_{LO}) with different LAPW basis parameters (see Table I for the significance of the notation used in the plot). The inset shows the results obtained using the ZnO-2 parameters but the Zn $3d$ states treated as core states by force.

To better understand the effects of HLOs for GW band gaps, it is instructive to have a look at how adding additional HLOs affects the KS single-particle spectrum. Figure 2(a) shows the band energies of ZnO at the Γ point ($\mathbf{k} = \mathbf{0}$) obtained with $n_{\mathrm{LO}} = 0$ (the default LAPW basis) and $n_{\mathrm{LO}} = 5$, respectively. A common feature of these two sets of data is that the energy of unoccupied states increases smoothly as a function of the band index (n) up to the plane-wave cutoff energy $\varepsilon^{\mathrm{PW}}_{\mathrm{max}}$ (36.0 Ry in the current case), and then it increases abruptly to much higher energy. With $n_{\mathrm{LO}} = 5$, the number of high-energy LO states beyond $\varepsilon^{\mathrm{PW}}_{\mathrm{max}}$ increases significantly. As shown in the inset of Fig. 2, while the KS band energies below 5 Ry are nearly unaffected by additional LOs, significant changes can be clearly observed in the energy of high-lying states (> 5 Ry), for which adding LOs tends to decrease the band energies. We note that a more detailed analysis on the effects of HLOs on

TABLE I. ZnO with different parameters, including muffin radii for Zn and O (in Bohr) and RK_{max}, used in the calculations. Zn $3p$ states are treated as semicore states by using LOs at the corresponding energy in all cases except ZnO-4, where they are treated as core states.

			n_{max}		$E_g(G_0W_0)$(eV)	
Notation	R_{MT}'s	RK_{max}	$n_{\mathrm{LO}}=0$	$n_{\mathrm{LO}}=8$	$n_{\mathrm{LO}}=0$	$n_{\mathrm{LO}}=8$
ZnO	(2.10, 1.50)	9.0	597	809	1.83	2.32
ZnO-1	(1.95, 1.70)	9.0	423	639	1.70	2.31
ZnO-2	(2.10, 1.50)	7.0	289	501	1.79	2.30
ZnO-3	(1.70, 1.20)	9.0	1156	1368	1.86	2.29
ZnO-4	(2.10, 1.50)	7.0	286	498	1.80	2.31

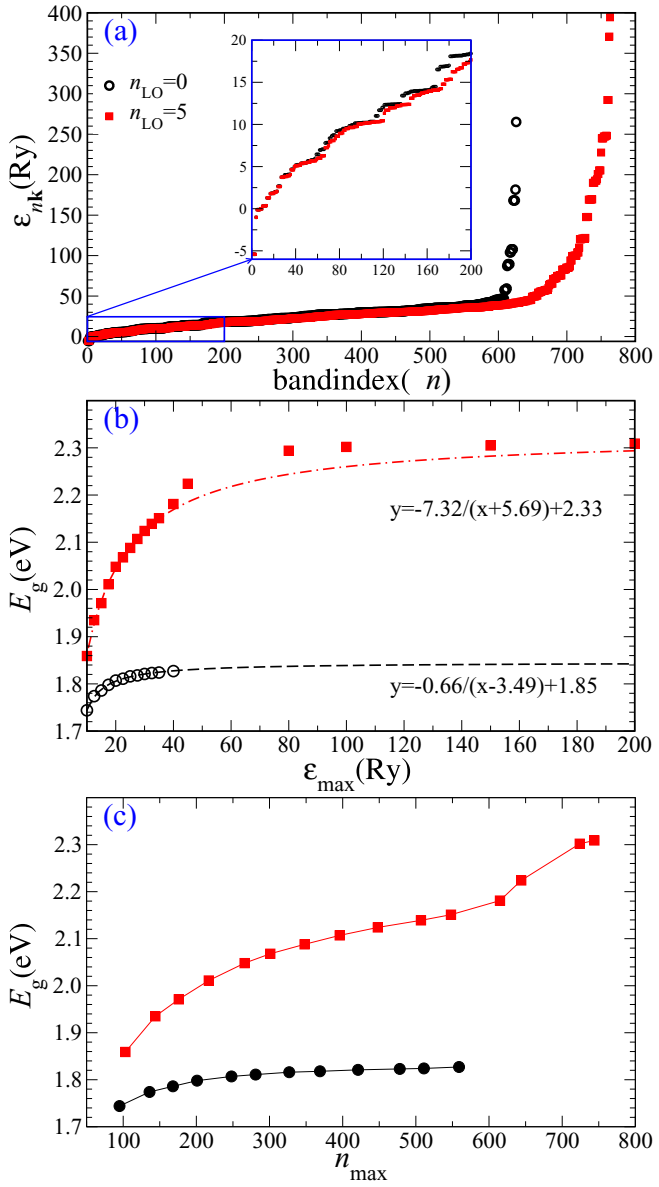

FIG. 2. (a) Comparison of Kohn-Sham band energies of ZnO at the Γ point [$\mathbf{k} = (0,0,0)$] obtained from using the default LAPW basis and those with additional high-energy local orbitals with $n_{LO} = 5$; (b) the convergence of the G_0W_0 band gap of ZnO (calculated with $N_k = 2 \times 2 \times 2$) as a function of ε_{max}^{GW}, the energy cutoff for the highest unoccupied states considered, with $n_{LO} = 0$ and $n_{LO} = 5$, respectively; and (c) the G_0W_0 band gap of ZnO as a function of n_{max}, the number of bands considered with $n_{LO} = 0$ and $n_{LO} = 5$, respectively.

Kohn-Sham states was already presented in Refs. [14] and [24] by Friedrich *et al.*, and therefore it is not repeated here.

We can therefore see that adding additional high-energy LOs has mainly two physical effects: (i) it improves the description of high-lying unoccupied stated by reducing the linearization error of the default LAPW basis, and (ii) it makes available additional especially high-energy states. It is obvious that those high-energy states are not "good" eigenstates of the Kohn-Sham Hamiltonian since they are well represented only within muffin-tin spheres by the LO basis functions. We will call them high-energy LO states in the following discussion. To see that both features in the effects of HLOs are important for the improvement of GW results, we compare how the G_0W_0 band gap of ZnO converges with respect to the energy cutoff for the highest unoccupied states considered in the GW calculations (ε_{max}^{GW}) with $n_{LO} = 0$ and 5, respectively, in Fig. 2(b). We also show the convergence of the G_0W_0 band gap as a function of the total number of states n_{max} in Fig. 2(c). When high-energy LO states are considered, the G_0W_0 band gap exhibits steplike features as a function of n_{max}, but it converges smoothly as a function ε_{max}^{GW}. When using the default LAPW basis ($n_{LO} = 0$), the G_0W_0 band gap converges quite quickly as ε_{max}^{GW} increases. In contrast, with $n_{LO} = 5$ it converges slowly when ε_{max}^{GW} is less than ε_{max}^{PW}, but it converges quickly when those high-energy LO states are considered, i.e., $\varepsilon_{max}^{GW} > \varepsilon_{max}^{PW}$. In the regime of $\varepsilon_{max}^{GW} < \varepsilon_{max}^{PW}$, the dependence of the G_0W_0 band gap on ε_{max}^{GW} can be well fitted by the following function:

$$E_g(x) = \frac{a}{x - \epsilon_0} + E_g^{\infty}, \tag{10}$$

which is similar to the fitting scheme used in Ref. [24] except that we use ε_{max}^{GW} instead of the number of unoccupied bands as the fitting variable. Using Eq. (10), the extrapolated G_0W_0 band gap corresponding to $\varepsilon_{max}^{GW} = \infty$ is 2.33 eV (for the $2 \times 2 \times 2$ **k**-mesh) using the data from $n_{LO} = 5$, which is remarkably close to the value of the G_0W_0 band gap (2.32 eV) obtained by considering all available states including those beyond the plane-wave cutoff. We can see that the consideration of high-energy LO states in the GW calculations, which is about 150 in terms of the number, has similar effects to the extrapolation to an infinite number of bands. In that sense, introducing HLOs in the LAPW basis can help to achieve the convergence of the G_0W_0 band gap with respect to the number of unoccupied states in a more efficient way. The fact that with $n_{LO} = 0$ the band gap obtained from the extrapolation to an infinite number of unoccupied states is still about 0.5 eV smaller than that from $n_{LO} = 5$ clearly indicates that both the accuracy of the conduction-band states within the plane-wave cutoff and the availability of the high-energy LO states beyond the plane-wave cutoff are crucial to obtain the numerically accurate G_0W_0 band gap.

In the preceding calculations, HLOs are added to both Zn and O atoms. We also perform calculations with HLOs only added to Zn or O, and a comparison of three different treatments (HLOs for both Zn and O, for Zn only, and for O only) is plotted in Fig. 3. Interestingly, the effects of HLOs on Zn and O are very different: for the O-only case, the band gap increases abruptly when n_{LO} increases from 0 to 1, and then it becomes quite flat as n_{LO} increases further, but for the Zn-only case, the band gap increases gradually and tends to converge only after $n_{LO} >\sim 5$. It is therefore clear that the slow convergence of the GW band gap of ZnO as a function of n_{LO} is mainly caused by Zn, which is likely to be related to the presence of the semicore $3d$ states. The role of Zn $3d$ states can be directly checked by performing a calculation of ZnO with Zn $3d$ states manually treated as part of a core, which removes all possible hybridization between Zn $3d$ and O $2p$ states. As shown in the inset of Fig. 1, the G_0W_0 band gap in this case becomes nearly constant as $n_{LO} \geqslant 2$.

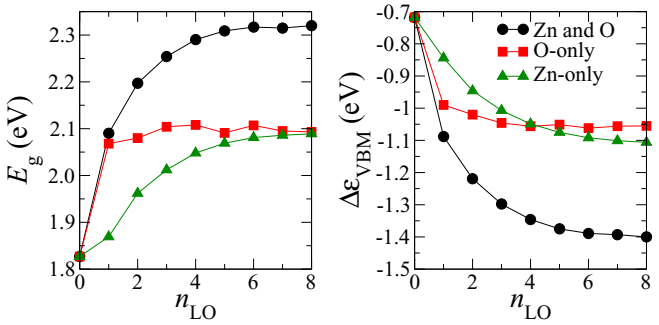

FIG. 3. The G_0W_0 band gap (left) and the correction to the VBM (right) in ZnO as a function of n_{LO} (calculated with $N_k = 2 \times 2 \times 2$).

As we mentioned in the Introduction, the other electronic property of great importance is the GW correction to the valence-band maximum ($\Delta\mathcal{E}_{VBM}$), which plays an important role in making an accurate determination of ionization potentials of semiconductors [40]. Figure 3 shows the $\Delta\mathcal{E}_{VBM}(G_0W_0)$ for ZnO as a function of n_{LO}, and it clearly shows that adding HLOs leads to a remarkable increase in the absolute values of $\Delta\mathcal{E}_{VBM}(G_0W_0)$, even more strongly than it does the band gap. The latter indicates that the effects of HLOs are different for the GW corrections to VBM and CBM states, and the VBM states are pushed toward lower energy more strongly than the CBM states. Similar features have been observed in several previous studies [22,25]. In Ref. [22], it was found that Coulomb-hole self-energies for the VBM and the CBM converge in a significantly different way as a function of the number of conduction bands (N_b) included in the calculations, which is attributed to the different characters of the VBM and CBM states [22].

B. Other typical cases

We further consider the effects of HLOs on G_0W_0 results in other typical insulating systems, again with a small **k**-mesh (see Sec. II C for details) to simplify the calculations. Figure 4 shows the results for ZnS and TiO_2. Since ZnS also has shallow semicore states, we expect similar slow convergence with respect to n_{LO}, which is true to some extent, although the overall dependence on n_{LO} is much weaker than that in ZnO.

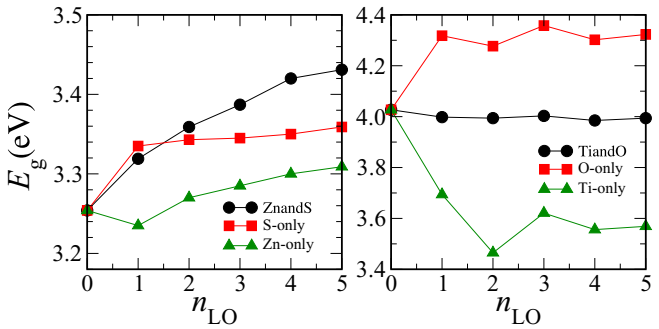

FIG. 4. Convergence of the G_0W_0 band gap of ZnS (left) and TiO_2 (right), calculated with $N_k = 2 \times 2 \times 2$ and $2 \times 2 \times 3$, respectively, as a function of the number of additional high-energy local orbitals (n_{LO}) with a different way of including HLOs.

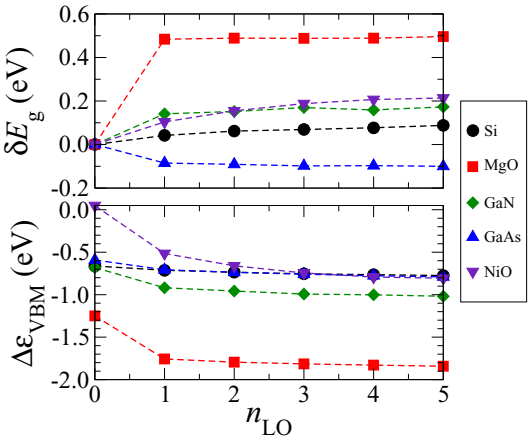

FIG. 5. Convergence of the G_0W_0 band gaps [$\delta E_g(n_{LO}) \equiv E_g(n_{LO}) - E_g(n_{LO} = 0)$], and G_0W_0 corrections to the VBM ($\Delta\mathcal{E}_{VBM}$) as a function of the number of additional high-energy local orbitals (n_{LO}) in typical compounds (calculated with $N_k = 2 \times 2 \times 2$).

The band gap from $n_{LO} = 5$ is only 0.18 eV larger than that from $n_{LO} = 0$. Similar to ZnO, when HLOs are added to the S atom only, the band gap increases significantly when n_{LO} increases from 0 to 1, and then it becomes nearly constant as n_{LO} increases further, but when HLOs are added to the Zn atom only, the band gap increases more gradually as a function of n_{LO}. The effects of HLOs in TiO_2 are very different from those in ZnO and ZnS, and the band gap decreases slightly ($\sim$0.03 eV) as n_{LO} increases to 5. By adding HLOs to O and Ti only, respectively, we can see that HLOs on the O atom still increase the band gap, but adding HLOs on the Ti atom actually reduces the band gap, such that when HLOs are added to both Ti and O, the band gap is nearly constant. The peculiar features in TiO_2 are likely related to the fact that the conduction band of TiO_2 is mainly of Ti $3d$ character, while the VBM has O $2p$ character. Adding O-HLOs reduces the VBM, while adding Ti-HLOs reduces mainly the CBM, thus the gap is fairly insensitive to HLOs. This is significantly different from ZnO, where the VBM is affected by both Zn and O HLOs, but the effects for the VBM are much larger than those for the CBM.

Figure 5 shows the G_0W_0 band gap as a function of n_{LO} in a few other typical insulators and semiconductors. For Si, the most significant change takes place when the first set of high-energy LOs are introduced ($n_{LO} = 1$), which increases the G_0W_0 gap by about 0.05 eV. Adding more LOs has a much weaker effect, and with $n_{LO} = 5$ an overall increase of about 0.1 eV is obtained, which is significantly smaller than that in ZnO. For MgO, a highly ionic insulator, the band gap first increases greatly by about 0.6 eV when n_{LO} increases from 0 to 1, and then it becomes nearly constant for bigger n_{LO}. For GaN, a highly ionic semiconductor, the G_0W_0 exhibits a similar dependence on n_{LO} as in MgO, but the overall effects are weaker. We also consider NiO as an example of transition-metal oxides, for which the G_0W_0 gap increases by about 0.2 eV when $n_{LO} = 5$ is used. For GaAs, interestingly, the band gap actually decreases by about 0.1 eV when HLOs are included. Overall we can see that the effects of HLOs on G_0W_0 are highly system-dependent.

TABLE II. Calculated band gaps (in eV) from different theoretical approaches for a selected set of prototypical semiconductors and insulators. The last three rows show the mean error (ME), mean absolute error (MAE), and mean absolute relative error (MARE) of results from different theoretical approaches with respect to experimental data that are mostly obtained from Refs. [50] and [55] (the averaged value is used for systems with several experimental data). To see the effects of LOs more explicitly, the differences between the results from GW_0 ($n_{\mathrm{LO}} = 0$) and GW_0 ($n_{\mathrm{LO}} = 5$), δE_g, are also shown. For systems with heavy elements, the effects of spin-orbit coupling are taken into account by a correction term Δ_{SO} that is calculated by PBE and given in parentheses together with the PBE band gaps. The last column collects the previously published PBE-based GW_0 band gaps using the norm-conserving projector augmented wave (NC-PAW) approach [56].

			G_0W_0	GW_0	G_0W_0	GW_0		GW_0 (NC-PAW)
Systems	Expt.	PBE	$n_{\mathrm{LO}} = 0$		$n_{\mathrm{LO}} = 5$		δE_g	(from Ref. [56])
C	5.48	4.16	5.49	5.66	5.69	5.87	0.21	5.81
Si	1.17	0.56	1.03	1.09	1.12	1.19	0.10	1.21
SiC	2.42	1.36	2.23	2.36	2.38	2.53	0.17	2.60
BN	6.4	4.46	6.04	6.27	6.36	6.61	0.34	6.66
BP	2.4, 2.1	1.34	2.01	2.09	2.11	2.20	0.11	
wz-AlN	6.2-6.3	4.14	5.60	5.88	5.80	6.11	0.23	
AlP	2.51	1.57	2.25	2.36	2.37	2.51	0.15	2.62
AlAs	2.1	1.34(0.10)	1.94	2.03	2.06	2.17	0.14	2.35
AlSb	1.6	1.03(0.22)	1.40	1.45	1.50	1.57	0.12	1.76
GaN	3.30	1.68	2.78	2.96	3.00	3.21	0.25	3.48
GaP	2.26	1.66	2.05	2.12	2.21	2.30	0.18	2.40
GaAs	1.42	0.42(0.11)	1.31	1.39	1.15	1.23	−0.16	1.21
GaSb	0.81	−0.12(0.23)	0.64	0.71	0.47	0.51	−0.20	0.51
InP	1.34	0.65	1.19	1.26	1.20	1.27	0.01	1.33
ZnO	3.4	0.70	2.05	2.41	2.78	3.32	0.91	
wz-ZnO	3.4	0.83	2.24	2.59	3.01	3.55	0.96	3.40
ZnS	3.68	2.07	3.15	3.35	3.35	3.61	0.26	3.72
ZnSe	2.7	1.15(0.13)	2.23	2.41	2.34	2.54	0.13	2.66
ZnTe	2.26	0.98(0.27)	1.95	2.08	1.89	2.02	−0.06	2.15
wz-CdS	2.49	1.20	2.02	2.18	2.19	2.38	0.20	
wz-CdSe	1.75	0.55(0.12)	1.29	1.42	1.39	1.54	0.12	1.60
CdTe	1.43	0.48(0.28)	1.20	1.30	1.23	1.34	0.04	1.44
MgS	4.5	2.79	4.10	4.32	4.24	4.48	0.16	
MgO	7.83	4.75	7.08	7.52	7.52	8.01	0.49	
LiF	14.20	9.28	12.36	13.98	14.27	15.13	1.15	
NaCl	8.5	5.12	7.67	8.15	7.92	8.43	0.28	
ME		−1.59	−0.47	−0.24	−0.23	0.01		
MAE		1.59	0.47	0.25	0.25	0.15		
MARE(%)		50	14	8	10	6		

Figure 5 also shows the GW corrections to the VBM in different systems. We see that in all cases, adding HLOs leads to a remarkable increase in the magnitude of $\Delta\mathcal{E}_{\mathrm{VBM}}$ and makes it more negative, even more strongly than it does the band gap. Again, the quantitative effects are strongly system-dependent and they appear to be larger for more ionic systems, since then the characters of the CBM and the VBM are even more different, and they are thus affected differently.

C. Benchmark results for semiconductors

We have shown that the G_0W_0 results for both band gaps and valence-band corrections can be significantly affected by improving the standard LAPW basis with HLOs. Therefore, the errors exhibited in many previously reported LAPW-based GW results [13,15–17,21] may be attributed to the inaccuracy of the normal LAPW basis instead of the inadequacy of the GW approach itself. In this section, we present both G_0W_0 and GW_0 results for a set of prototypical insulating systems calculated using well-converged computational parameters with the numerical errors estimated to be smaller than 0.05 eV. The main results, collected in Table II, exhibit some general trends. In general, the systems with light elements are more strongly affected by the consideration of HLOs. For binary semiconductors with the same cationic species, such as GaX (X = N, P, As, and Sb) and ZnX (X = O, S, Se, and Te), the change of the GW_0 band gap due to the inclusion of HLOs, $\delta E_{\mathrm{g}} \equiv E_{\mathrm{g}}(GW_0, n_{\mathrm{LO}} = 5) - E_{\mathrm{g}}(GW_0, n_{\mathrm{LO}} = 0)$, decreases systematically as the atomic number of X increases, and it even becomes negative for GaAs, GaSb, and ZnTe. On the other hand, for the binary semiconductor series with the same anionic species, such as MN (M = B, Al, and Ga), with δE_{g} being 0.34, 0.23, and 0.25 eV, respectively, or MP (M = B, Al, Ga, and InP), with δE_{g} being 0.11, 0.15, 0.18, and 0.01 eV, respectively, the dependence on the nature of the cationic species is more complicated. It is also interesting to

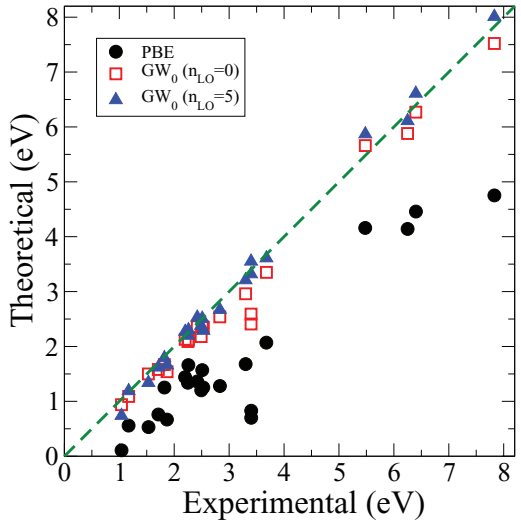

FIG. 6. GW_0 band gaps of a set of prototypical semiconductors and insulators obtained with $n_{\mathrm{LO}} = 0$ and 5 against experimental data. The averaged value is used for systems with several experimental data.

note that δE_g for the isoelectronic series Si-AlP-MgS-NaCl (0.10, 0.15, 0.16, and 0.28 eV, respectively) exhibits some dependence on the material's ionicity. We have therefore confirmed that indeed ZnO is one of the rare extreme cases for which an adequate consideration of high-lying unoccupied states is critical to obtain numerically accurate GW results.

To evaluate the performances of different theoretical approaches, the mean error (ME), the mean absolute error (MAE), and the mean absolute relative error (MARE) of theoretical results with respect to experimental values are calculated and shown in the last rows of Table II. To show the accuracy of different theoretical approaches more clearly, Fig. 6 plots the band gaps from PBE, GW_0 ($n_{\mathrm{LO}} = 0$) and GW_0 ($n_{\mathrm{LO}} = 5$), against the experimental values. We note in passing that as far as the band gap is concerned, the comparison between theory and experiment has to be undertaken with caution. The experimental band gap of a given material can depend on a lot of factors, including the particular experimental approach used for the measurement (photoemission spectroscopy, optical absorption, or electric transport), the sample quality, the conditions (in particular, the temperature) in which it is measured, the way the band gap is extracted from the experimental spectral data, and last but not least, the involvement of other physical effects such as electron-hole (excitonic) [5] and electron-phonon (polaronic) [64] coupling effects, which are not considered in typical electronic-structure theoretical approaches. In general, the consideration of HLOs significantly reduces the errors of the GW calculations. In particular, GW_0 with $n_{\mathrm{LO}} = 5$ leads to a MAE of only 0.15 eV and a MARE of 6%, which is already comparable to the uncertainty in the experimental data of normal semiconductors.

We have shown that the consideration of HLOs can significantly change the GW correction to the valence-band maximum $\Delta\mathcal{E}_{\mathrm{VBM}}$. The latter can be used to correct the ionization potentials obtained from PBE-based slab model calculations (see Ref. [40] for more details). Table III collects

TABLE III. Calculated ionization potentials from the PBE slab model calculation and those with the GW corrections. The last two rows show the mean absolute error (MAE) and mean absolute relative error (MARE) of results from different theoretical approaches with respect to experimental data (the averaged value is used for systems with several experimental data).

		$n_{\mathrm{LO}} = 0$		$n_{\mathrm{LO}} = 5$		
Systems	PBE	G_0W_0	GW_0	G_0W_0	GW_0	Expt.
Si	4.88	5.37	5.46	5.57	5.71	5.10,[a] 5.25,[b] 5.35[c]
Ge	4.22	4.47	4.51	4.76	4.86	4.80,[a] 4.74[d]
GaN	5.98	6.68	6.85	7.16	7.45	7.5[f]
GaP	5.32	5.70	5.77	6.00	6.16	6.01[g]
GaAs	4.74	5.20	5.28	5.48	5.65	5.47,[a] 5.56[g]
GaSb	4.23	4.65	4.72	4.88	5.02	4.91,[g] 4.76[a]
ZnO	6.13	7.05	7.36	8.08	8.69	7.82[h]
ZnS	6.13	6.85	7.01	7.34	7.66	7.5[h]
ZnSe	5.57	6.24	6.38	6.69	6.97	6.82[h]
ZnTe	4.94	5.53	5.65	5.89	6.12	5.75[h]
CdS	6.04	6.71	6.86	7.08	7.35	7.26[h]
CdSe	5.55	6.00	6.10	6.42	6.64	6.62[h]
CdTe	4.98	5.46	5.56	5.81	6.01	5.78[h]
MAE	0.97	0.44	0.33	0.14	0.24	
MARE(%)	14.9	6.7	5.1	2.2	3.8	

[a]Reference [57].
[b]Reference [58].
[c]Reference [59].
[d]Reference [60].
[e]Reference [60].
[f]Reference [61].
[g]Reference [62].
[h]Reference [63].

the ionization potentials of a selected set of semiconductors from PBE and different variants of GW approaches, where PBE results are already reported in Ref. [40]. In general, we can see that the consideration of HLOs improves the agreement with experiment, which is most significant for systems with shallow semicore d states. Apparently, the G_0W_0 results for the IPs are in slightly better agreement with experiment than GW_0 after HLOs are considered. The IPs from GW_0 tend to be overestimated compared to experimental values, which is consistent with the findings in Ref. [41]. On the other hand, considering the error bars and the limited number of experimental data, we cannot make an unambiguous judgment on which approach is more accurate.

We close this section by making some comparison between our results and previously published ones, especially those that have been carefully calibrated in terms of numerical accuracy [25]. In particular, Kresse and co-workers [25,41,56] have carefully investigated the band gaps of many semiconductors that are also considered in this work by using the GW approach implemented in the projector augmented wave (PAW) basis with approximately norm-conserving (NC) partial waves, hence termed NC-PAW in the following. The latter can significantly improve the description of unoccupied states up to about 30 Ry above the Fermi energy. In addition, the convergence with respect to the number of unoccupied states is also carefully monitored by systematically increasing the

energy cutoff for the states considered in the GW calculations and extrapolating the results to an infinite basis-set limit. The last column of Table II shows the GW_0 band gaps obtained in the NC-PAW approach. We can see that the agreement between the NC-PAW results and ours [GW_0 ($n_{\mathrm{LO}} = 5$)] is surprisingly good, with the differences in most cases being about 0.1 eV, which is remarkable considering the dramatic differences in the implementation details of the two approaches. Nevertheless, there are still some noticeable differences. For most of the semiconductors with shallow semicore d states, the GW_0 gaps in the NC-PAW approach are usually larger by about 0.1 eV than ours, but for wz-ZnO the opposite is observed. Two factors may contribute to these differences. First, in the PAW-based implementation of the GW approach, the core-valence interactions are treated at the exchange-only level [9], while our LAPW-based implementation considers the full core-valence interactions. Secondly, as previously mentioned, for systems such as ZnO, the inclusion of HLOs to the LAPW basis with the angular momentum number l up to 6 is necessary to obtain numerically well-converged results, which means that in the PAW approach one needs to include PAW projectors beyond valence l-channels, which are normally used, to achieve similar numerical accuracy.

IV. CONCLUDING REMARKS

To summarize, in this work we have presented a systematic investigation on the effects of including high-energy local orbital basis functions in the LAPW-based GW prediction of quasiparticle electronic band structures of semiconductors. Using ZnO as the representative, we show that the effects of HLOs are twofold: on the one hand, they improve the description of high-lying unoccupied states, and on the other hand, they provide access to a few hundred extremely high-energy states, a consideration of which in GW calculations can help to effectively achieve the numerical convergence for the summation of unoccupied states. By investigating the effects of HLOs included only for Zn and O atoms, respectively, we see that the slow convergence of the GW band gap of ZnO can be attributed mainly to the presence of Zn 3d states. In addition to ZnO, we also investigated the convergence of GW band gaps with respect to the number of HLOs for several other typical systems. We found that the effects of HLOs are highly system-dependent, and in most cases the band gap changes by less than 0.2 eV with the inclusion of HLOs. In contrast, HLOs have even stronger effects on the GW correction to the valence-band maximum, which is of great significance for the GW prediction of the ionization potentials of semiconductors. Considering the significant effects of HLOs on the GW results, it is important to reevaluate the performances of GW based on a more accurate numerical treatment. For that purpose, we have considered an extended set of semiconductors whose experimental band gaps are relatively well established. We found that in general using a HLO-enhanced LAPW basis significantly improves the agreement with experiment for both the band gap and the ionization potential, and overall the partially self-consistent GW approach, GW_0, gives an optimal performance.

We close the paper with some general remarks, especially with regard to the recent debates on the GW band gap of ZnO. Although our work addresses the effects of including HLOs for GW calculations based on the LAPW basis, our findings are nevertheless of general significance. We have shown that the inclusion of HLOs improves both the accuracy and the completeness of unoccupied states considered in the GW calculation. Our findings indicate that the accuracy of unoccupied states that are more than tens of eV above the Fermi level has significant effects on quasiparticle energies around the Fermi level. Currently widely used pseudopotentials (PPs), either in the norm-conserving (NC), ultrasoft (US), or PAW schemes, are all constructed by requiring that the valence states are well described, which implies that unoccupied states with energy far away from the Fermi level may not be accurately treated even with a large cutoff for the plane-wave basis. This may explain the fact that Stankovski *et al.* [23], when using the more accurate contour deformation approach [2] to the frequency dependence, still obtain a rather small G_0W_0 band gap of ZnO even with the well-converged plane-wave basis and a larger number of unoccupied states. In the PAW framework, Kresse and co-workers [41] have developed more sophisticated pseudoization procedures to build approximately norm-conserving PAW potentials that can significantly improve the accuracy of unoccupied states. Using the NC-PAW approach, the band gap of wz-ZnO from GW_0@PBE is 3.40 eV [56], which is very close to the value of 3.55 eV obtained in this work. Regarding the issue of achieving completeness in the summation of unoccupied states, Refs. [24] and [41] used the extrapolation technique to obtain numerically converged GW band gaps, which is inconvenient in practice. Our investigations of ZnO have shown that the results obtained by taking all states available with a given HLO-extended LAPW basis agree very well with those from the extrapolation. The remarkable role of HLOs in achieving basis-set completeness may well be generalized to other implementations of GW, including, in particular, those based on an atomiclike local basis [65].

ACKNOWLEDGMENTS

We acknowledge helpful discussion with Robert Laskowski and Xinguo Ren. This work is partly supported by the National Natural Science Foundation of China (Projects No. 21173005, No. 21211130098, No. 21373017, and No. 21321001) and the Ministry of Education (20120001110063), and the Ministry of Science and Technology (2013CB933400, 2011CB201402). P.B. was supported by the Austrian Science Fund (FWF) project SFB F41 (ViCoM).

[1] M. S. Hybertsen and S. G. Louie, Phys. Rev. B **34**, 5390 (1986).

[2] R. W. Godby, M. Schlüter, and L. J. Sham, Phys. Rev. B **37**, 10159 (1988).

[3] F. Aryasetiawan and O. Gunnarsson, Rep. Prog. Phys. **61**, 237 (1998).

[4] W. G. Aulbur, L. Jönsson, and J. W. Wilkins, in *Solid State Physics*, edited by H. Ehrenreich and F. Spaepen (Academic Press, New York, 2000), Vol. 54, p. 1.

[5] G. Onida, L. Reining, and A. Rubio, Rev. Mod. Phys. **74**, 601 (2002).

[6] M. Rohlfing, P. Krüger, and J. Pollmann, Phys. Rev. B **48**, 17791 (1993).

[7] H. N. Rojas, R. W. Godby, and R. J. Needs, Phys. Rev. Lett. **74**, 1827 (1995).

[8] S. Lebègue, B. Arnaud, M. Alouani, and P. E. Bloechl, Phys. Rev. B **67**, 155208 (2003).

[9] M. Shishkin and G. Kresse, Phys. Rev. B **74**, 035101 (2006).

[10] F. Aryasetiawan, Phys. Rev. B **46**, 13051 (1992).

[11] W. Ku and A. G. Eguiluz, Phys. Rev. Lett. **89**, 126401 (2002).

[12] T. Kotani and M. van Schilfgaarde, Solid State Commun. **121**, 461 (2002).

[13] M. Usuda, N. Hamada, T. Kotani, and M. van Schilfgaarde, Phys. Rev. B **66**, 125101 (2002).

[14] C. Friedrich, A. Schindlmayr, S. Blügel, and T. Kotani, Phys. Rev. B **74**, 045104 (2006).

[15] M. van Schilfgaarde, T. Kotani, and S. V. Faleev, Phys. Rev. B **74**, 245125 (2006).

[16] R. Gomez-Abal, X. Li, M. Scheffler, and C. Ambrosch-Draxl, Phys. Rev. Lett. **101**, 106404 (2008).

[17] C. Friedrich, S. Blügel, and A. Schindlmayr, Phys. Rev. B **81**, 125102 (2010).

[18] H. Jiang, R. I. Gomez-Abal, X. Li, C. Meisenbichler, C. Ambrosch-Draxl, and M. Scheffler, Comput. Phys. Commun. **184**, 348 (2013).

[19] M. Rohlfing, P. Krüger, and J. Pollmann, Phys. Rev. B **57**, 6485 (1998).

[20] M. L. Tiago, S. Ismail-Beigi, and S. G. Louie, Phys. Rev. B **69**, 125212 (2004).

[21] X.-Z. Li, R. Gomez-Abal, H. Jiang, C. Ambrosch-Draxl, and M. Scheffler, New J. Phys. **14**, 023006 (2012).

[22] B.-C. Shih, Y. Xue, P. Zhang, M. L. Cohen, and S. G. Louie, Phys. Rev. Lett. **105**, 146401 (2010).

[23] M. Stankovski, G. Antonius, D. Waroquiers, A. Miglio, H. Dixit, K. Sankaran, M. Giantomassi, X. Gonze, M. Côté, and G.-M. Rignanese, Phys. Rev. B **84**, 241201(R) (2011).

[24] C. Friedrich, M. C. Müller, and S. Blügel, Phys. Rev. B **83**, 081101(R) (2011).

[25] J. Klimes, M. Kaltak, and G. Kresse, Phys. Rev. B **90**, 075125 (2014).

[26] In the GW_0 approach, the screened Coulomb interaction W is fixed to that calculated from the reference Kohn-Sham orbital energies and wave functions (W_0), but the Green's function G is self-consistently calculated with quasiparticle energies. See, e.g., Refs. [18] and [27] for more details.

[27] M. Shishkin and G. Kresse, Phys. Rev. B **75**, 235102 (2007).

[28] F. Fuchs, J. Furthmüller, F. Bechstedt, M. Shishkin, and G. Kresse, Phys. Rev. B **76**, 115109 (2007).

[29] H. Dixit, R. Saniz, D. Lamoen, and B. Partoens, J. Phys. Condens. Matter **22**, 125505 (2010).

[30] A. Schleife, C. Rödl, F. Fuchs, J. Furthmüller, and F. Bechstedt, Phys. Rev. B **80**, 035112 (2009).

[31] L. Y. Lim, S. Lany, Y. J. Chang, E. Rotenberg, A. Zunger, and M. F. Toney, Phys. Rev. B **86**, 235113 (2012).

[32] P. Rinke, A. Qteish, J. Neugebauer, C. Freysoldt, and M. Scheffler, New. J. Phys. **7**, 126 (2005).

[33] M. van Schilfgaarde, T. Kotani, and S. Faleev, Phys. Rev. Lett. **96**, 226402 (2006).

[34] M. Shishkin, M. Marsman, and G. Kresse, Phys. Rev. Lett. **99**, 246403 (2007).

[35] D. J. Singh, Phys. Rev. B **43**, 6388 (1991).

[36] D. J. Singh and L. Nordström, *Planewaves, Pseudopotentials and the LAPW Method*, 2nd ed. (Springer, New York, 2006).

[37] H. Jiang, J. Chem. Phys. **134**, 204705 (2011).

[38] M. C. Toroker, D. K. Kanan, N. Alidoust, L. Y. Isseroff, P. Liao, and E. A. Carter, Phys. Chem. Chem. Phys. **13**, 16644 (2011).

[39] H. Jiang, J. Phys. Chem. C **116**, 7664 (2012).

[40] H. Jiang and Y.-C. Shen, J. Chem. Phys. **139**, 164114 (2013).

[41] A. Grüneis, G. Kresse, Y. Hinuma, and F. Oba, Phys. Rev. Lett. **112**, 096401 (2014).

[42] V. Stevanovic, S. Lany, D. S. Ginley, W. Tumas, and A. Zunger, Phys. Chem. Chem. Phys. **16**, 3706 (2014).

[43] P. Blaha, K. Schwarz, G. K. H. Madsen, D. Kvasnicka, and J. Luitz, *WIEN2k, An Augmented Plane Wave + Local Orbitals Program for Calculating Crystal Properties* (Tech. Universitat Wien, Austria, 2001).

[44] R. Laskowski and P. Blaha, Phys. Rev. B **85**, 035132 (2012).

[45] R. Laskowski and P. Blaha, Phys. Rev. B **89**, 014402 (2014).

[46] E. E. Krasovskii and W. Schattke, Solid State Commun. **93**, 775 (1995).

[47] E. E. Krasovskii, Phys. Rev. B **56**, 12866 (1997).

[48] M. Betzinger, C. Friedrich, S. Blügel, and A. Görling, Phys. Rev. B **83**, 045105 (2011).

[49] G. Michalicek, M. Betzinger, C. Friedrich, and S. Blügel, Comput. Phys. Commun. **184**, 2670 (2013).

[50] T. Chiang, K. Frank, H. Freund, A. Goldmann, F. J. Himpsel, U. Karlsson, R. Leckey, and W. Schneider, *Landolt-Börnstein, New Series, III/23a: Electronic Structure of Solids: Photoemission Spectra and Related Data* (Springer, 1989).

[51] See Supplemental Material at http://link.aps.org/supplemental/10.1103/PhysRevB.93.115203 for additional computational details and data.

[52] G. K. H. Madsen, P. Blaha, K. Schwarz, E. Sjöstedt, and L. Nordström, Phys. Rev. B **64**, 195134 (2001).

[53] J. P. Perdew, K. Burke, and M. Ernzerhof, Phys. Rev. Lett. **77**, 3865 (1996).

[54] In an erratum (Ref. [66]) to Ref. [24], Friedrich *et al.* claimed that by considering the second-order derivative LO in the SCF calculation, the LDA gap of wz-ZnO decreases from 0.84 to 0.73 eV, and the G_0W_0 gap decreases from 2.99 to 2.83 eV. But in our calculations using WIEN2K, the LDA gap using the default LAPW basis (corresponding to $n_{\mathrm{LO}} = 0$) is 0.75 eV. Adding one HLO per l for $l = 0$–3 in SCF ($n_{\mathrm{LO}} = 1$), which should be numerically equivalent to using the second-order derivative LOs as in the work of Friedrich *et al.*, only changes the LDA gap to 0.74 eV. In the case of PBE, using $n_{\mathrm{LO}} = 1$ in SCF changes the band gap from 0.83 to 0.82 eV. Apparently in WIEN2K, the default LAPW basis is already accurate enough for LDA/GGA SCF calculations. We also note that our LDA and PBE gaps agree quite well with the PAW results (LDA: 0.75 eV from Ref. [25]

and PBE: 0.80 eV from Ref. [56]). We have also done *GW* calculations using HLO-improved PBE effective potentials, and their effects on the *GW* results are also marginal.

[55] O. Madelung, *Semiconductors: Data Handbook*, 3rd ed. (Springer-Verlag, New York, 2004).

[56] Y. Hinuma, A. Grüneis, G. Kresse, and F. Oba, Phys. Rev. B **90**, 155405 (2014).

[57] G. W. Gobeli and F. G. Allen, Phys. Rev. **137**, A245 (1965).

[58] F. J. Himpsel, G. Hollinger, and R. A. Pollak, Phys. Rev. B **28**, 7014 (1983).

[59] C. Sebenne, D. Bolmont, G. Guichar, and M. Balkanski, Phys. Rev. B **12**, 3280 (1975).

[60] G. Guichar, G. A. Garry, and C. Sebenne, Surf. Sci. **85**, 326 (1979).

[61] J. I. Pankove and H. Schade, Appl. Phys. Lett. **25**, 53 (1974).

[62] J. van Laar, A. Huijser, and T. L. van Rooy, J. Vac. Sci. Technol. **14**, 894 (1977).

[63] R. K. Swank, Phys. Rev. **153**, 844 (1967).

[64] M. Cardona and M. L. W. Thewalt, Rev. Mod. Phys. **77**, 1173 (2005).

[65] X. Ren, P. Rinke, V. Blum, J. Wieferink, A. Tkatchenko, A. Sanfilippo, K. Reuter, and M. Scheffler, New J. Phys. **14**, 053020 (2012).

[66] C. Friedrich, M. C. Müller, and S. Blügel, Phys. Rev. B **84**, 039906(E) (2011).